

An Adaptive Observer-based Robust Estimator of Multi-sinusoidal Signals

Boli Chen, Gilberto Pin, Wai M. Ng, S. Y. Ron Hui and Thomas Parisini

Abstract—This paper presents an adaptive observer-based robust estimation methodology of the amplitudes, frequencies and phases of biased multi-sinusoidal signals in presence of bounded perturbations on the measurement. The parameters of the sinusoidal components are estimated on-line and the update laws are individually controlled by an excitation-based switching logic enabling the update of a parameter only when the measured signal is sufficiently informative. This way doing, the algorithm is able to tackle the problem of over-parametrization (i.e., when the internal model accounts for a number of sinusoids that is larger than the true spectral content) or temporarily fading sinusoidal components. The stability analysis proves the existence of a tuning parameter set for which the estimator’s dynamics are input-to-state stable with respect to bounded measurement disturbances. The performance of the proposed estimation approach is evaluated and compared with other existing tools by extensive simulation trials and real-time experiments.

I. INTRODUCTION

The identification of the amplitude, frequency and phase (AFP) of a signal composed by a single or multiple sinusoids is one of the fundamental issues arising in a variety of practical applications, such as, for example, power quality monitoring, vibration control and periodic disturbance rejection. In the literature, currently there does not exist a multi-sinusoidal estimator with semi-global stability properties and robustness – in an ISS sense – with respect to bounded unstructured perturbations when the number of sinusoids is possibly over-estimated.

Usually, the Fast Fourier Transform (FFT) is preferred for its efficiency in stationary conditions (i.e., when the frequency content is constant within the considered time-window) and for its simple structure. However, the accuracy drops in the case of time-varying frequencies. In this respect, a number of methods have been conceived to provide online detection of

the time-varying amplitude/frequency (see, for example, [1], [2], [3], [4] and references cited therein). Among them, it is worth to recall the adaptive notch-filtering method (ANF) (see [5], [6]) and the Phase-Locked-Loop (PLL) (see, for instance [7], [8]) for their popularity in power and electrical systems, though they are applicable for a single sinusoid only. In several practical applications, a zero-mean sinusoidal signal is not available; to deal with a dc offset, the traditional PLL and ANF methodologies are typically augmented heading towards a second-order generalized integrator-based orthogonal signal generator (OSG-SOGI) [9]. The OSG-SOGI architecture is also exploited in [10] and [11] to cope with the biased signal case, namely, in [11] the OSG-SOGI is extended to the third-order generalized integrator-based OSG (OSG-TOGI) that is characterized by an adaptive resonant frequency. Apart from the aforementioned methods, a number of nonlinear estimation algorithms employing suitable pre-filtering techniques also have been presented in literature to address the AFP estimation in presence of an unknown bias (see, for example, [12], [13], [14], [15], [16] and the references cited therein).

Recent research efforts have been devoted to the detection of harmonics and inter-harmonics (multiple sinusoids). Based on the PLL and ANF approach, the estimation of the parameters of multi-sinusoidal signals are dealt with by linking multiple PLL and ANF units in parallel. In [17] and [18], the AFP estimation of two independent sinusoidal components are addressed resorting to two PLL-based blocks with a decorrelator factor that specializes in discriminating two nearby frequencies. Following the preliminary work [19] concerning harmonically constructed signal with ANFs in parallel, an improved framework handling the n inter-harmonics is reported in [20] that is shown advantageous from a computational perspective with respect to the counterpart relying on multiple PLLs (see [21]). A variant of the OSG-TOGI scheme called adaptive frequency-locked-Loop (AFL) filter based TOGI has been recently presented in [22], in which the explicit contents of the multi-sinusoidal signal can be tracked by deploying a bank of AFL filters. In spite of the direct frequency estimation, only local stability can be guaranteed for the aforementioned PLL by averaging methods.

The adaptive observer is another key methodology exploited to track multiple frequencies because of its notable feature in terms of stability: global or semi-global stability is ensured in most cases (see [23], [24], [25], [26], [27] and [28]). In particular, [26] presents a simplified global stability analysis by using contraction theory rather than traditional Lyapunov analysis; and, on the other hand, [28] proposes a hybrid observer to identify the n frequencies from a multi-frequency

The dissemination of this work is being supported by the European Union’s Horizon 2020 research and innovation programme under grant agreement No 739551 (KIOS CoE).

B. Chen is with the Dept. of Electrical and Electronic Engineering at the Imperial College London, UK (boli.chen10@imperial.ac.uk).

G. Pin is with Electrolux Italia S.p.A, Italy, e-mail: (gilbertopin@alice.it).

W. M. Ng is with the Dept. of Electrical and Electronic Engineering, The University of Hong Kong, Hong Kong (wmng@eee.hku.hk).

S. Y. R. Hui is with the Dept. of Electrical and Electronic Engineering, The University of Hong Kong, Hong Kong, and also with the Dept. of Electrical and Electronic Engineering at the Imperial College London, UK (ronhui@eee.hku.hk; r.hui@imperial.ac.uk).

T. Parisini is with the Dept. of Electrical and Electronic Engineering at the Imperial College London, UK, with the KIOS Research and Innovation Centre of Excellence, University of Cyprus, and also with the Dept. of Engineering and Architecture at the University of Trieste, Italy (t.parisini@gmail.com).

signal with saturated amplitudes. Recently, the effectiveness of the hybrid observer in the presence of poorly sampled signal is shown in [29].

Moreover, the possible bias term in the measurement can be handled by suitably augmenting the adaptive observer system (see [30], [31], [32]). However, the observer-based approaches rely on a certain linear parameterization to incorporate the unknown frequencies into a state space representation of the measured signal; in such cases, the estimated frequencies are usually not directly estimated. Instead, the parameter adaptation laws regard a set of coefficients of the characteristic polynomial of the autonomous signal generator system and the true frequencies act as the zeros of the characteristic polynomial, the computation of which might result in an excessive computational burden that may severely limit the online applicability.

In the spirit of prior work by the authors on the single sinusoidal case (see the very recent paper [33]), a “dual-mode” estimation scheme is proposed, which incorporates a switching algorithm depending on the instantaneous excitation level (concerning the excitation issues, a related contribution focusing on switching or hybridization to improve persistence of excitation can be found in [?]). In contrast with other methods that are either indirectly identifying the frequency contents or are characterized by local stability only, the present paper deals with a direct adaptation mechanism for the squares of the frequencies with semi-global stability based on the recent preliminary results presented in [34]. Moreover, the robustness to the bounded measurement noise, that is likely to appear in real-world applications, is addressed by Input-to-State-Stability (ISS) arguments. It is shown that the ISS property with respect to the additive measurement noise is ensured by suitably choosing a few suitable tuning parameters. In comparison with [34], the proposed novel estimator adopts a n -dimensional excitation-based switching signal to separately control the multiple frequency adaptation in all directions by means of suitable matrix decomposition techniques, thus enhancing the practical implementation and avoiding unnecessarily disabled adaptation in the scenario that only parts of the directions fulfill the excitation condition (e.g., over-parametrization scenarios).

The paper is organized as follows: Section II introduces the AFP problem in the multi-sinusoidal signal scenario. In Section III, the adaptive observer-based estimator is proposed. Then, the stability analysis is dealt with in Section IV. Finally, simulation and real experimental results showing the effectiveness of the algorithm are given in Section V.

II. PROBLEM FORMULATION AND PRELIMINARIES

Consider the following perturbed multi-sinusoidal signal:

$$\begin{cases} \hat{y}(t) = A_0 + \sum_{i=1}^n A_i \sin(\varphi_i(t)) + d(t), \\ \dot{\varphi}_i(t) = \omega_i \end{cases} \quad (1)$$

with $\varphi_i(0) = \varphi_{0_i}$, where A_0 is an unknown constant bias, the amplitudes of the sinusoids verify the inequality $A_i \geq 0, \forall i \in \{1, \dots, n\}$, φ_{0_i} is the unknown initial phase of

each sinusoid, and the frequencies are strictly-positive time-invariant parameters: $\omega_i > 0, \omega_i \neq \omega_j$ for $i \neq j$. The term $d(t)$ represents an additive measurement disturbance, bounded by a known (possibly conservative) constant $\bar{d} > 0$, such that $|d(t)| < \bar{d}, \forall t \in \mathbb{R}_{\geq 0}$.

Now, let us denote by $y(t)$ the noise-free signal

$$y(t) = A_0 + \sum_{i=1}^n A_i \sin(\omega_i t + \varphi_{0_i}) \quad (2)$$

which is assumed to be generated by the following observable autonomous marginally-stable dynamical system:

$$\begin{cases} \dot{x}(t) = F_x x(t) + \sum_{i=1}^n F_i x(t) \theta_i^* \\ y(t) = C_x x(t) \end{cases} \quad (3)$$

with $x(t) \triangleq [x_1(t), \dots, x_{2n+1}(t)]^\top \in \mathbb{R}^{2n+1}$ and where $x(0) = x_0$ represents the unknown initial condition. The new parametrization $\theta_1^*, \dots, \theta_n^*$ used in (3) is related to the original frequency parameters by

$$\theta_i^* = a_i + \Omega_i, \quad \forall i \in \{1, \dots, n\}, \quad (4)$$

with $\Omega_i = \omega_i^2, \forall i \in \{1, \dots, n\}$ and where a_1, a_2, \dots, a_n are non-zero constants designed with the only requirements to satisfy $a_i \in \mathbb{R}, a_i \neq a_j$ for $i \neq j$. The matrices of the linear biased multi-oscillator (3) are given by

$$F_x = \begin{bmatrix} J_1 & 0_{2 \times 2} & \cdots & 0_{2 \times 2} & 0 \\ 0_{2 \times 2} & J_2 & \ddots & 0_{2 \times 2} & 0 \\ \vdots & \ddots & \ddots & \ddots & \vdots \\ 0_{2 \times 2} & \ddots & \ddots & J_n & 0 \\ 0 & \cdots & \cdots & 0 & 0 \end{bmatrix}, \quad C_x^\top = \begin{bmatrix} c_1^\top \\ c_2^\top \\ \vdots \\ c_n^\top \\ 1 \end{bmatrix},$$

where $0_{m \times n}$ represents a $m \times n$ null matrix,

$$J_i = \begin{bmatrix} 0 & 1 \\ a_i & 0 \end{bmatrix}, \quad c_i = [1 \quad 0].$$

Moreover, each F_i in system (3) is a square matrix having the $(2i, 2i-1)$ th entry equal to -1 . Defining

$$J_0 = \begin{bmatrix} 0 & 0 \\ -1 & 0 \end{bmatrix},$$

F_1 and F_2 take on, for instance, the form:

$$F_1 = \begin{bmatrix} J_0 & 0_{2 \times (2n-1)} \\ 0_{(2n-1) \times 2} & 0_{(2n-1) \times (2n-1)} \end{bmatrix},$$

$$F_2 = \begin{bmatrix} 0_{2 \times 2} & 0_{2 \times 2} & 0_{2 \times (2n-3)} \\ 0_{2 \times 2} & J_0 & 0_{2 \times (2n-3)} \\ 0_{(2n-3) \times 2} & 0_{(2n-3) \times 2} & 0_{(2n-3) \times (2n-3)} \end{bmatrix}.$$

Thanks to (3), the noisy signal $\hat{y}(t)$ can be thought as generated by the observable system

$$\begin{cases} \dot{x}(t) = F_x x(t) + G_x(x(t)) \theta^* \\ \hat{y}(t) = C_x x(t) + d(t) \end{cases} \quad (5)$$

with $x(0) = x_0$ and where

$$G_x(x(t)) = [G_{x_1}(x(t)) \cdots G_{x_i}(x(t)) \cdots G_{x_n}(x(t))], \quad (6)$$

$$G_{x_i}(x(t)) = [0_{1 \times (2i-1)} \quad x_{2i-1}(t) \quad 0_{1 \times (2n+1-2i)}]^\top, \\ \forall i = 1, 2, \dots, n, \quad (7)$$

and $\theta^* \in \mathbb{R}^n$ denotes the true parameter vector $[\theta_1^* \dots \theta_n^*]^\top$.

In the following, we are going to show that the system (5) verifies all the requirements needed for the application of the switched-observer based methodology developed by the authors in [35]. On the other hand, in order to cope with the over-parametrization issue (i.e., the model is established with a number of sinusoids-parameters that is larger than the number of the components of the actual signal), the adaptation mechanism presented in [35] is completely re-designed in this paper, thus enabling the adaptation of the sole frequencies for which enough excitation is detected based on instantaneous checking of the excitation level.

Remark 2.1: The elements of $G_x(\cdot)$ are globally Lipschitz continuous functions, that is:

$$\|G_x(x') - G_x(x'')\| \leq |x' - x''|, \forall x', x'' \in \mathbb{R}^{2n+1}.$$

Moreover, the true state $x(t)$ is norm-bounded for any initial condition, i.e. $|x(t)| \leq \bar{x}, \forall t \in \mathbb{R}_{\geq 0}$. Both the Lipschitz condition on $G_x(\cdot)$ and the bound \bar{x} allow to establish the following further bound

$$\|G_x(x(t))\| \leq \bar{x}, \forall t \in \mathbb{R}_{\geq 0}.$$

In the next section, the adaptive-observer scheme to compute the estimates $\hat{x}(t)$ and $\hat{\theta}(t)$ will be described. Hence, for the time-being, let us suppose $\hat{x}(t)$ and $\hat{\theta}(t)$ to be available. Then, the full AFP estimates are obtained by

$$\hat{\Omega}_i(t) = \hat{\theta}_i(t) - a_i, \quad \hat{\omega}_i(t) = \sqrt{\hat{\theta}_i(t) - a_i}, \quad (8)$$

$$\hat{A}_i(t) = \sqrt{\left(\hat{\Omega}_i(t)\hat{x}_{2i-1}(t)^2 + \hat{x}_{2i}(t)^2\right) / \hat{\Omega}_i(t)}, \quad (9)$$

and

$$\hat{\varphi}_i(t) = \angle(\hat{x}_{2i}(t) + j\hat{\omega}_i(t)\hat{x}_{2i-1}(t)), \quad i = 1, 2, \dots, n. \quad (10)$$

In addition, the offset is evaluated directly by $\hat{A}_0 = \hat{x}_{2n+1}$. It worth noting that (9) is not well-defined at the time instants t in which $\hat{\Omega}_i(t) = 0$. In spirit of the previous work by the authors on the estimation of a single sinusoidal signal [33], this limitation can be removed resorting to a suitable adaptive mechanism based on gradient method. More specifically, by defining the time-varying residual based on the equality (9):

$$R_i(\hat{A}_i(t), t) \triangleq \hat{A}_i(t)\hat{\omega}_i(t) - \sqrt{\hat{\Omega}_i(t)\hat{x}_{2i-1}(t)^2 + \hat{x}_{2i}(t)^2},$$

then, the following adaptation law can be designed:

$$\dot{\hat{A}}_i(t) = \begin{cases} 0, & \text{if } \hat{A}_i(t) = 0 \text{ and } \dot{\hat{A}}_i(t) < 0 \\ \dot{\hat{A}}_i(t), & \text{otherwise} \end{cases}$$

where

$$\dot{\hat{\alpha}}_i(t) = -\mu_A \frac{\partial R_i(\hat{A}_i(t), t)}{\partial \hat{A}_i(t)} R_i(\hat{A}_i(t), t) \\ = -\mu_A \hat{\omega}_i(t) \left[\hat{\omega}_i(t)\hat{A}_i(t) - \sqrt{\left(\hat{\Omega}_i(t)\hat{x}_{2i-1}(t)^2 + \hat{x}_{2i}(t)^2\right)} \right] \quad (11)$$

with $\hat{A}_i(0) = 0$. $\mu_A \in \mathbb{R}_{>0}$ denotes a tuning gain set by the designer to ensure the asymptotic convergence of $R_i(\hat{A}_i(t), t)$ to 0.

In order to proceed with the analysis, the following further assumption is needed.

Assumption 1: The frequencies of the sinusoids are bounded by a positive constant $\bar{\omega}$, such that $\omega_i < \bar{\omega}, \forall i \in \{1, \dots, n\}$.

According to Assumption 1, there exists a known positive constant θ^* , such that $|\theta^*| \leq \theta^*$. More specifically, in the remaining parts of the paper we consider $\theta^* \in \Theta^*$, where $\Theta^* \subset \mathbb{R}^n$ is a hypersphere of radius θ^* .

III. FILTERED-AUGMENTATION-BASED ADAPTIVE OBSERVER

Now, we are going to generalize the switched-mode adaptive observer preliminarily proposed in [35] to the biased multi-oscillator (5). Specifically, let us augment the dynamics of the observed system with a synthetic low-pass filter driven by the noisy measurement vector:

$$\dot{\hat{y}}_f(t) = F_f \hat{y}_f(t) + B_f \hat{y}(t), \quad (12)$$

where F_f and B_f are fixed by the designer such that F_f is Hurwitz and the pair (F_f, B_f) is controllable. $\hat{y}_f(t) \in \mathbb{R}^{n_f}$ denotes the accessible state vector and with arbitrary initial condition \hat{y}_{f0} , such that the dimension n_f of the augmented dynamics verifies $n_f = n - 1$.

For the sake of the forthcoming analysis, it is convenient to split the filtered output into two components:

$$\hat{y}_f(t) = y_f(t) + d_f(t),$$

where $y_f(t)$ and $d_f(t)$ can be thought as produced by two virtual filters, driven by the unperturbed output and by the measurement disturbance respectively:

$$\dot{y}_f(t) = F_f y_f(t) + B_f y(t) \quad (13)$$

and

$$\dot{d}_f(t) = F_f d_f(t) + B_f d(t). \quad (14)$$

Consequently, in view of (5), (13) and (14), the overall augmented system dynamics with the extended perturbed output measurement equation can be written as follows:

$$\begin{cases} \dot{z}(t) = F_z z(t) + G_z(z(t))\theta^* \\ \eta(t) = C_z z(t) \\ \dot{\hat{\eta}}(t) = \eta(t) + d_\eta(t) \end{cases} \quad (15)$$

with $z(0) = z_0 \in \mathbb{R}^{n_z}$, $n_z = 2n + 1 + n_f = 3n$, and $z(t) \triangleq [x^\top(t) \ y_f^\top(t)]^\top$, $z_0 \triangleq [x_0^\top(t) \ y_{f0}^\top]^\top$, $\hat{\eta}(t) \triangleq$

$$[\hat{y}(t) \hat{y}_f^\top(t)]^\top, d_\eta(t) \triangleq [d(t) d_f^\top(t)]^\top$$

$$F_z \triangleq \begin{bmatrix} F_x & 0_{(2n+1) \times (n-1)} \\ B_e C_x & F_f \end{bmatrix},$$

$$C_z \triangleq \begin{bmatrix} C_x & 0_{1 \times (n-1)} \\ 0_{(n-1) \times (2n+1)} & I_{(n-1)} \end{bmatrix},$$

and

$$G_z(z(t)) \triangleq \begin{bmatrix} G_x(T_{zx}z(t)) \\ 0_{(n-1) \times n} \end{bmatrix},$$

with the transformation matrix given by $T_{zx} \triangleq [I_{2n+1} \ 0_{(2n+1) \times (n-1)}]$. It is worth noting that $G_z(z(t))$ is also Lipschitz, with unitary Lipschitz constant as $G_x(x(t))$, and can be norm-bounded by \bar{x} . Moreover, the assumed norm-bound \bar{d} on the output noise implies the existence of \bar{d}_η such that $\bar{d}_\eta > 0 : |d_\eta(t)| \leq \bar{d}_\eta, \forall t \in \mathbb{R}_{\geq 0}$.

Now, we introduce the structure of the adaptive observer for joint estimation of $z(t)$ and θ^* in (15), and in turn estimating the frequencies $\hat{\Omega}_i, i = 1, \dots, n$. Besides the measured output filter (12), the architecture of the estimator also includes three dynamic components (16), (17) and (19), which are described below:

1) *Augmented state estimator:*

$$\dot{\hat{z}}(t) = (F_z - LC_z)\hat{z}(t) + L\hat{\eta}(t) + G_z(\hat{z}(t))\hat{\theta}(t) + \Xi(t)\hat{\theta}(t) \quad (16)$$

with $\hat{z}(0) = \hat{z}_0$ and where $\Xi(t)$ is defined in (18). The gain matrix L is given by

$$L \triangleq \begin{bmatrix} L_x & 0_{(2n+1) \times (n-1)} \\ 0_{(n-1) \times 1} & 0_{(n-1) \times (n-1)} \end{bmatrix}$$

where L_x is a suitable gain matrix such that $F_x - L_x C_x < 0$.

2) *Parameter-affine state-dependent filters:*

Let $G_{z_1}(z(t)), \dots, G_{z_n}(z(t))$ be the columns of $G_z(z(t))$, that is

$$G_z(z(t)) = [G_{z_1}(z(t)) \ \dots \ G_{z_i}(z(t)) \ \dots \ G_{z_n}(z(t))].$$

Then, we introduce a set of auxiliary signal $\xi_i(t), i = 1, \dots, n$, whose dynamics obeys the following differential equations driven by the available (estimated) counterpart of $G_z(z(t))$:

$$\dot{\xi}_i(t) = (F_z - LC_z)\xi_i(t) + G_{z_i}(\hat{z}(t)), \forall i = 1, \dots, n, \quad (17)$$

with $\xi_i(0) = 0_{n_z \times 1}$. By collecting all the filters' states, let us also define an auxiliary signal matrix

$$\Xi(t) = [\xi_1(t) \ \dots \ \xi_i(t) \ \dots \ \xi_n(t)]. \quad (18)$$

3) *Frequency adaptation unit:*

Herein, a projection operator \mathcal{P} is utilized to confine the estimated parameter $\hat{\theta}(t)$ to the predefined convex region Θ^*

$$\hat{\theta}(t) = \mathcal{P} \left[\hat{\theta}_{unc}(\Psi(t), t) \right]_{|\hat{\theta}| \leq \bar{\theta}^*} \quad (19)$$

with $\hat{\theta}(0) = \hat{\theta}_0$ set arbitrarily, and where $\hat{\theta}_{unc}$ is the unconstrained parameter's derivative, whose explicit expression is given in (22); $\Psi(t) \in \mathbb{R}^{n \times n}$ represents a diagonal matrix

consisting of binary (1: on, 0: off) on-off switching signals which enable or disable the adaptation of a specific parameter

$$\Psi(t) \triangleq \text{diag}[\psi_1(t), \dots, \psi_i(t), \dots, \psi_n(t)], \quad (20)$$

with the adaptation-enabling signals $\psi_i(t), \forall i = 1, 2, \dots, n$ specified later on. For brevity, in the sequel we will write $\hat{\theta}_{unc}(t)$ instead of $\hat{\theta}_{unc}(\Psi(t), t)$, dropping the dependence of $\hat{\theta}_{unc}$ on $\Psi(t)$. The parameters' derivative projection operator in (19) is defined as:

$$\mathcal{P} \left[\hat{\theta}_{unc}(t) \right]_{|\hat{\theta}| \leq \bar{\theta}^*} \triangleq \begin{cases} \text{nsp}(\hat{\theta}^\top(t)) \left(\text{nsp}(\hat{\theta}^\top(t)) \right)^\top \hat{\theta}_{unc}(t), \\ \quad \text{if } |\hat{\theta}| = \bar{\theta}^* \text{ and } \hat{\theta}^\top(t) \hat{\theta}_{unc}(t) > 0 \\ \hat{\theta}_{unc}(t), \text{ otherwise} \end{cases}$$

in which $\text{nsp}(\cdot)$ denotes the null-space of a row vector. The projection can be expressed as

$$\hat{\theta}(t) = \hat{\theta}_{unc}(t) - \mathcal{I}(\theta) \frac{\hat{\theta}(t) \hat{\theta}^\top(t)}{\bar{\theta}^{*2}} \hat{\theta}_{unc}(t) \quad (21)$$

where $\mathcal{I}(\theta)$ denotes the indicator function given by

$$\mathcal{I}(\theta) \triangleq \begin{cases} 1, & \text{if } |\hat{\theta}(t)| = \bar{\theta}^* \text{ and } \hat{\theta}^\top(t) \hat{\theta}_{unc}(t) > 0, \\ 0, & \text{otherwise.} \end{cases}$$

Now, the unconstrained derivative is given by:

$$\dot{\hat{\theta}}_{unc}(t) \triangleq -\mu U_\Psi(t) (\Psi(t) S_\Psi(t)) U_\Psi^\top(t) U_\Xi(t) \check{S}_\Xi(t) U_\Xi^\top(t) \times \Xi^\top(t) C_z^\top (C_z \hat{z}(t) - \hat{\eta}(t)), \quad (22)$$

with $U_\Psi, S_\Psi, U_\Xi, \check{S}_\Xi$ defined in the following. The matrices U_Ψ and S_Ψ are obtained by the SVD of $\Phi_\Psi(\Xi(t))$:

$$\begin{aligned} \Phi_\Psi(\Xi(t)) &= (\Xi^\top(t) \Xi(t) + \rho^2 I)^{-1} \Xi^\top(t) C_z^\top C_z \Xi(t) \\ &= U_\Psi(t) S_\Psi(t) U_\Psi^\top(t) \end{aligned} \quad (23)$$

in which $S_\Psi(t)$ is a diagonal matrix comprising all the eigenvalues of $\Phi_\Psi(\Xi(t))$. Analogously, U_Ξ and S_Ξ are obtained by the SVD of the matrix $\Phi_\Xi(\Xi)$ defined as:

$$\Phi_\Xi(\Xi(t)) \triangleq \Xi^\top(t) C_z^\top C_z \Xi(t) = U_\Xi(t) S_\Xi(t) U_\Xi^\top(t).$$

Thanks to the above decomposition, let us define the matrix $\check{S}_\Xi(t) \triangleq \text{diag} \{ \check{s}_{\Xi_i}(t) \}$ where

$$\check{s}_{\Xi_i}(t) = \begin{cases} \lambda_i (S_\Xi(t))^{-1}, & \text{if } \psi_i(t) = 1, \\ 0, & \text{if } \psi_i(t) = 0 \end{cases} \quad (24)$$

where $\lambda_i(\cdot)$ is the notation for i th eigenvalue. We assign the following hysteretic dynamics to the binary switching signal $\psi_i(t), i = 1, 2, \dots, n$ that determines the activation/suppression of the parameter adaptation:

$$\psi_i(t) = \begin{cases} 1, & \text{if } \lambda_i(\Phi_\Psi(\Xi(t))) \geq \bar{\delta} \\ 0, & \text{if } \lambda_i(\Phi_\Psi(\Xi(t))) < \underline{\delta} \\ \psi_i(t^-), & \text{if } \underline{\delta} \leq \lambda_i(\Phi_\Psi(\Xi(t))) < \bar{\delta} \end{cases} \quad (25)$$

The transition thresholds $\underline{\delta}, \bar{\delta}$ are designed such that $0 < \underline{\delta} < \bar{\delta} < 1$.

It is worth noting that the above hysteresis strategy ensures a

minimum finite duration between transitions (see Section IV-C for a detailed discussion) and hence a suitable dwell-time. In the next section, the stability of the proposed switching mechanism is characterized to analytically determine a dwell-time, in turn depending on the signals to be estimated, the adaptation gains and the transition thresholds. Clearly, introducing hysteresis is not the only way to ensure the presence of a dwell-time and other alternatives are available like, for instance, the introduction of a suitable delay.

The detailed pseudocode for the proposed algorithm is given in Algorithm 1 illustrated below.

Remark 3.1: To avoid the possible interference between the estimators (e.g., two or more estimators to converge to the same frequency value), we may apply distinct frequency ‘clips’ in different ranges of frequency based on a priori knowledge on the nominal frequency values (a similar idea of frequency separation can be found in [20]).

Algorithm 1 Algorithm for the proposed estimator

Parameters: tuning parameters

$a_i, F_f, B_f, \mu, \rho, \mu_A, \bar{\delta}, \underline{\delta}$, sampling time T_s , simulation time T and the poles;

Initialization: Define the initial condition of the estimated variables, $\hat{x}, \hat{\theta}$ while L_x is determined by pole placement;

1: Calculate parameters F_z, C_z, L for the augmented system;

LOOP Process

- 2: **for** $k = 1$ to $N = T/T_s$ **do**
 - 3: Calculate the filtered signal $\hat{y}_f(k)$ using (12);
 - 4: Calculate the state estimate $\hat{z}(k)$ using (16), $\hat{x}(k)$ is part of $\hat{z}(k)$ and the estimated bias is $\hat{A}_0(k) = \hat{x}_{2n+1}(k)$;
 - 5: Calculate the auxiliary signals $\xi_i(k)$ using (17);
 - 6: Collect all the filters’ states to get auxiliary signal matrix $\Xi(k)$ using (18);
 - 7: Calculate $\Phi_\Psi(\Xi(k))$ using (23) and the associated eigenvalues by SVD;
 - 8: **if** $(\lambda_i(\Phi_\Psi(\Xi(k))) \geq \bar{\delta})$ **then**
 - 9: $\psi_i(k) = 1$;
 - 10: **else if** $(\lambda_i(\Phi_\Psi(\Xi(k))) < \underline{\delta})$ **then**
 - 11: $\psi_i(k) = 0$;
 - 12: **else**
 - 13: $\psi_i(k) = \psi_i(k - 1)$;
 - 14: **end if**
 - 15: Calculate $S_{\Xi}(k)$ from the SVD of $\Phi_{\Xi}(\Xi(k))$;
 - 16: Calculate $\tilde{S}_{\Xi}(k)$ based on $\psi_i(k)$ using (24) and $\tilde{S}_{\Xi}(k) \triangleq \text{diag} \{ \tilde{s}_{\Xi_i}(k) \}$;
 - 17: Calculate parameter estimate $\hat{\theta}(k)$ using (21) and (22);
 - 18: Calculate the amplitude, frequency and phase estimates $\hat{A}_i(k), \hat{\omega}_i(k), \hat{\varphi}_i(k)$ using (11), (8), (10), respectively;
 - 19: Reconstruct the sinusoidal signals by $\hat{y}(k) = \hat{A}_0(k) + \sum_{i=1}^n \hat{A}_i(k) \sin(\hat{\varphi}_i(k))$;
 - 20: **end for**
 - 21: **return** $\hat{A}_i, \hat{\omega}_i, \hat{\varphi}_i$ and \hat{y} .
-

IV. STABILITY ANALYSIS

In order to carry out the stability analysis, let us define the augmented state-estimation error vector

$$\tilde{z}(t) \triangleq \hat{z}(t) - z(t).$$

Moreover, in order to address the case of overparametrization (that is, the number of model parameters n is larger than the number of sinusoids $n_e(t) \in \mathbb{N} : 0 \leq n_e(t) \leq n$ that at time t are adapted), it is convenient to define two parameter estimation errors, one accounting for all the parameters

$$\tilde{\theta}(t) \triangleq \hat{\theta}(t) - \theta^* \in \mathbb{R}^n,$$

and the other considering the $n_e(t)$ components that are adapted at a given instant

$$\tilde{\theta}_{n_e(t)}(t) \triangleq \hat{\theta}_{n_e(t)}(t) - \theta_{n_e(t)}^* \in \mathbb{R}^{n_e(t)},$$

where $\hat{\theta}_{n_e(t)}(t)$ and $\theta_{n_e(t)}^*$ collect all and only those scalar components of the estimated and true parameter vectors for which $\psi_i(t) = 1$. In this connection, let $E_{n_e(t)} \in \mathbb{N}^{n_e(t)}$ be a set containing the integer indexes of all and only those components for which the adaptation is enabled at time t .

As said above, the case of overparametrization corresponds to a situation in which the number of frequency parameters of the observer, n , is larger than n_e , the number of non-zero amplitude sinusoids with unique frequency forming the measured signal¹ (more details of overparametrization in the context of adaptive control can be found in [36]). In this case a minimal realization of the generator of the measured signals is a multi-harmonic oscillator of order $2n_e$, composed by the collection of exactly n_e unique harmonic oscillators [37]. Nonetheless, a non-minimal realization for such a signal generator can be taken as the union of the said minimal multi-harmonic oscillator with an augmented dynamics formed by $(n - n_e)$ harmonic oscillators with null-states and arbitrary frequency. The possibility to assign arbitrarily the frequency of the augmented null-amplitude multi-oscillator is the key for proving the stability in this context. For the sake of the further discussion, without loss of generality, let us take the frequency parameters of the augmented dynamics equal to the present estimates produced by the filter for the components not adapted due to poor excitation, achieved by

$$\theta_i^* = \hat{\theta}_i(t), \forall i \in \{1, 2, \dots, n\} \setminus E_{n_e(t)}, \quad (26)$$

which implies

$$\tilde{\theta}_i(t) \triangleq \hat{\theta}_i(t) - \theta_i^* = 0, \forall i \in \{1, 2, \dots, n\} \setminus E_{n_e(t)}. \quad (27)$$

For the sake of the further discussion let us also define the linear time-varying combination of state and parameter vectors $\tilde{\zeta}(t) \triangleq \sum_{i=1}^n \xi_i(t) \tilde{\theta}_i(t) - \tilde{z}(t)$, The state-estimation

¹The residual sinusoidal signals not accounted for by the adaptation are masked and implicitly treated as a disturbance.

error evolves according to the differential equation:

$$\begin{aligned}\dot{\tilde{z}}(t) &= (F_z - LC_z)\tilde{z}(t) + Ld_\eta(t) + G_z(\tilde{z}(t))\tilde{\theta}(t) \\ &\quad + G_z(z(t))\tilde{\theta}(t) + G_z(\tilde{z}(t))\theta^* + \sum_{i=1}^n \xi_i(t)\dot{\tilde{\theta}}_i(t) \\ &= (F_z - LC_z)\tilde{z}(t) + Ld_\eta(t) + G_z(\tilde{z}(t))\theta^* \\ &\quad + \sum_{i \in E_{n_e}(t)} G_{z_i}(\tilde{z}(t))\tilde{\theta}_i(t) + \Xi(t)\dot{\tilde{\theta}}(t),\end{aligned}\quad (28)$$

where $G_z(\tilde{z}(t)) \triangleq G_z(\hat{z}(t)) - G_z(z(t))$. Meanwhile, the auxiliary variable $\tilde{\zeta}(t)$ evolves according to

$$\dot{\tilde{\zeta}}(t) = \sum_{i \in E_{n_e}(t)} \dot{\xi}_i(t)\tilde{\theta}_i(t) + \Xi(t)\dot{\tilde{\theta}}(t) - \dot{\tilde{z}}(t), \quad (29)$$

which, after some algebra, leads to

$$\begin{aligned}\dot{\tilde{\zeta}}(t) &= \sum_{i \in E_{n_e}(t)} \left((F_z - LC_z)\xi_i(t)\tilde{\theta}_i(t) + G_{z_i}(\hat{z}(t))\tilde{\theta}_i(t) \right) \\ &\quad + \Xi(t)\dot{\tilde{\theta}}(t) - (F_z - LC_z)\tilde{z}(t) - G_z(\tilde{z}(t))\tilde{\theta}(t) \\ &\quad - Ld_\eta(t) - G_z(z(t))\tilde{\theta}(t) - G_z(\tilde{z}(t))\theta^* - \Xi(t)\dot{\tilde{\theta}}(t) \\ &= (F_z - LC_z)\tilde{\zeta}(t) - Ld_\eta(t) - G_z(\tilde{z}(t))\theta^*.\end{aligned}\quad (30)$$

In Fig. 1, we draw the overall excitation-based switching scheme, which is instrumental for the forthcoming analysis. More specifically, let $k_e(t)$ be a counter for the transitions to

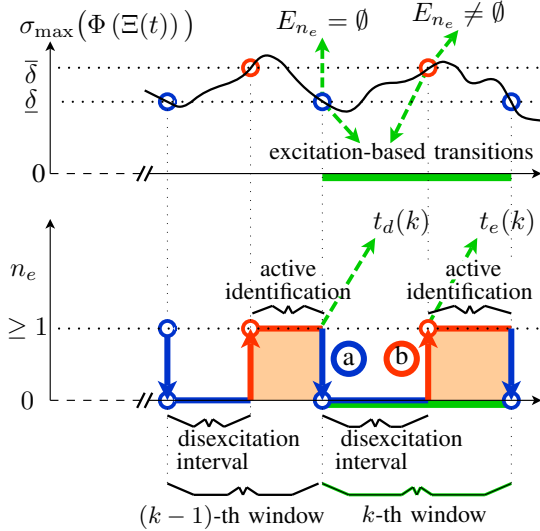


Fig. 1. Scheme of the excitation-based switching scheme for enabling/disabling the parameter adaptation. The transitions to dis-excitation (a) and to active identification phases (b) have been highlighted.

excitation, described by the jump dynamics given below:

$$k_e(t) = \begin{cases} k_e(t^-) + 1, & \text{if } E_{n_e}(t^-) = \emptyset \text{ and } E_{n_e}(t) \neq \emptyset, \\ k_e(t^-), & \text{if } E_{n_e}(t^-) \neq \emptyset \text{ and } E_{n_e}(t) = \emptyset. \end{cases}$$

Analogously, let $k_{1 \rightarrow 0}(t)$ be a counter with respect to the transition from excitation to dis-excitation:

$$k_d(t) = \begin{cases} k_d(t^-) + 1, & \text{if } E_{n_e}(t^-) \neq \emptyset \text{ and } E_{n_e}(t) = \emptyset, \\ k_d(t^-), & \text{if } E_{n_e}(t^-) = \emptyset \text{ and } E_{n_e}(t) \neq \emptyset. \end{cases}$$

Moreover, let $t_d(k)$ and $t_e(k)$ denote the transition time-

instants:

$$\begin{aligned}t_e(k) &\triangleq \inf(t \geq 0 : k_e(t) = k), \\ t_d(k) &\triangleq \inf(t \geq 0 : k_d(t) = k).\end{aligned}$$

Without loss of generality and taking into account that the system starts from zero-excitement, then

$$t_e(k) > t_d(k), \forall k \in \mathbb{Z}^+.$$

and the counters are initialised by $k_e(0) = 0, k_d(0) = 1$. Hence, the integer k always identifies a two-phase time-window made up of a dis-excitation interval followed by an active estimation interval (see Fig. 1).

Since $(F_z - LC_z)$ is Hurwitz, for any positive definite matrix Q , there exists a positive definite matrix P that solves the linear Lyapunov equation

$$(F_z - LC_z)^\top P + P(F_z - LC_z) = -2Q.$$

In the following, we will analyze the behaviour of the adaptive observer in two situations by a Lyapunov candidate that accounts for all the parameters:

$$V(t) \triangleq \frac{1}{2}(\tilde{z}^\top(t)P\tilde{z}(t) + \tilde{\theta}^\top(t)\tilde{\theta}(t) + g\tilde{\zeta}^\top(t)P\tilde{\zeta}(t)), \quad (31)$$

where $g \in \mathbb{R}_{>0}$.

i) Active adaptation interval of finite duration, i.e. in which $n_e(t) \geq 1 = n_e, \forall t \in [t_e(k), t_d(k+1)]$ (we will omit the time-dependence of n_e assuming that for the whole interval it remains constant). In this case the set $E_{n_e}(t)$ is non-empty, $V(t)$ defined in (31) shrinks to the following positive definite function, considering the sole components actively adapted:

$$V_{n_e}(t) \triangleq \frac{1}{2}(\tilde{z}^\top(t)P\tilde{z}(t) + \tilde{\theta}_{n_e}^\top(t)\tilde{\theta}_{n_e}(t) + g\tilde{\zeta}^\top(t)P\tilde{\zeta}(t)). \quad (32)$$

In this interval, we will prove that V_{n_e} is an ISS-Lyapunov function for the system comprising all states and only the parameters undergoing adaptation, that will converge to the true values. The present scenario comprises, besides the over-parametrization case, also the full-parametrization case, which yields to the ISS of the whole dynamics.

ii) Total dis-excitation, i.e., none of the parameters is adapted due to poor excitation. In this scenario the set $E_{n_e}(t)$ is empty. In this case we will show that the overall function (31) will remain bounded.

After that, the Lyapunov analysis in these two scenarios are linked properly and we are able to prove that the alternate occurrence of active identification phases and poorly excited phases yields to convergence, provided that the active identification phases have a sufficient duration. To simplify the analysis, we will consider that the number of adapted sinusoids n_e is fixed within a whole excitation/dis-excitation interval (see Fig. 1), that is the set $E_{n_e}(t)$ may be either the empty set $\{0\}$ during the dis-excitation phase, either a set $E_{n_e} \neq \emptyset$ for an arbitrary active adaptation interval (invariant set). Note that this assumption does not limit the applicability of the adaptive observer to this very special case, being it just a technicality needed to render the problem tractable in a simple analytical way (an active adaptation phase with time-varying $n_e(t)$ can be regarded as a combination of multiple excited intervals).

A. Active adaptation interval of finite duration

Consider an arbitrary active identification phase $t_e(k) \leq t < t_d(k+1)$ (see Fig. 1) and let $\Psi_{n_e}(t)$ be the binary matrix in this scenario with only $\psi_i(t) = 1, \forall i \in E_{n_e}$. The upcoming analysis is carried out in order to exhibit the benefit of using the derivative projection on the parameters' estimates. Thanks to (21), in presence of the projection $\mathcal{I}(\theta) = 1$ and $|\hat{\theta}(t)| = \bar{\theta}^*$, we have

$$\begin{aligned}\bar{\theta}^\top(t)\dot{\hat{\theta}}(t) &= \bar{\theta}^\top(t)\dot{\hat{\theta}}_{unc}(t) - \bar{\theta}^\top(t)\frac{\hat{\theta}(t)\hat{\theta}^\top(t)}{\bar{\theta}^{*2}}\dot{\hat{\theta}}_{unc}(t) \\ &= \bar{\theta}^\top(t)\dot{\hat{\theta}}_{unc}(t) - \frac{1}{\bar{\theta}^{*2}}\bar{\theta}^\top(t)\hat{\theta}(t)\hat{\theta}^\top(t)\dot{\hat{\theta}}_{unc}(t).\end{aligned}$$

Owing to the convexity of the admissible set, it holds that

$$\bar{\theta}^\top(t)\hat{\theta}(t) = \left(\hat{\theta}^\top(t) - \theta^{*\top}\right)\hat{\theta}(t) \geq 0.$$

Now, we recall the triggering condition of projection $\hat{\theta}^\top(t)\dot{\hat{\theta}}_{unc}(t) > 0$, which implies that

$$\frac{1}{\bar{\theta}^{*2}}\bar{\theta}^\top(t)\hat{\theta}(t)\hat{\theta}^\top(t)\dot{\hat{\theta}}_{unc}(t) \geq 0.$$

Finally, we can bound the scalar product $\bar{\theta}^\top(t)\dot{\hat{\theta}}(t)$ by:

$$\bar{\theta}^\top(t)\dot{\hat{\theta}}(t) = \bar{\theta}^\top(t)\dot{\hat{\theta}}(t) \leq \bar{\theta}^\top(t)\dot{\hat{\theta}}_{unc}(t).$$

For instance, a 2-dimensional pictorial representation of the projection-based adaptation is shown in Fig. 2 to enhance the influence of the derivative projection on the parameters estimates.

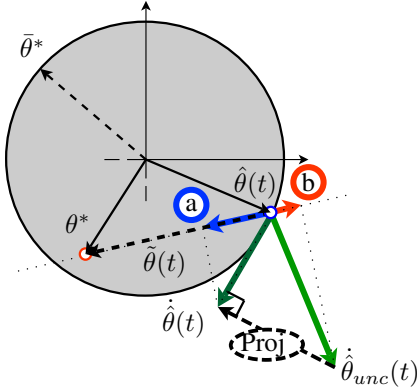


Fig. 2. 2D pictorial representation of the projection-based adaptation. When $|\hat{\theta}(t)| = \bar{\theta}^*$ and $\hat{\theta}_{unc}(t)$ points out of the feasible region, then the derivative of the parameter vector is obtained by projecting $\hat{\theta}_{unc}(t)$ to the tangential hyperplane. To visually compare the values of the scalar products $-\bar{\theta}^\top\dot{\hat{\theta}}_{unc}(t)$ and $-\bar{\theta}^\top\dot{\hat{\theta}}(t)$, consider the projected vectors (a) and (b) respectively.

In virtue of the fact that

$$\begin{aligned}U_\Psi(t)(\Psi_{n_e}(t)S_\Psi(t))U_\Psi^\top(t) &= (\Xi^\top(t)\Xi(t) + \rho^2I)^{-1} \\ &\times U_\Xi(t)(\Psi_{n_e}(t)S_\Xi(t))U_\Xi^\top(t)\end{aligned}$$

the unconstrained derivative $\dot{\hat{\theta}}_{unc}(t)$ can be expanded as fol-

lows:

$$\begin{aligned}\dot{\hat{\theta}}_{unc}(t) &= -\mu(\Xi^\top(t)\Xi(t) + \rho^2I)^{-1} \\ &\times U_\Xi(t)(\Psi_{n_e}(t)S_\Xi(t))U_\Xi^\top(t)U_\Xi(t)\check{S}_\Xi(t)U_\Xi^\top(t) \\ &\times \Xi^\top(t)C_z^\top(C_z\Xi(t)\tilde{\theta}(t) - d_\eta(t) - C_z\check{\zeta}(t)) \\ &= -\mu(\Xi^\top(t)\Xi(t) + \rho^2I)^{-1}\Psi_{n_e}(t)\Xi^\top(t)C_z^\top \\ &\times (C_z\Xi(t)\tilde{\theta}(t) - d_\eta(t) - C_z\check{\zeta}(t)).\end{aligned}\quad (33)$$

Thanks to (27) and let $\bar{c} \triangleq \|C_z\|$, the following inequality holds in presence of over-parametrization:

$$\begin{aligned}\frac{d}{dt}(\bar{\theta}_{n_e}^\top(t)\tilde{\theta}_{n_e}(t)) &\leq -\mu\delta|\tilde{\theta}_{n_e}(t)|^2 + \frac{\mu\bar{c}}{2\rho}|\tilde{\theta}_{n_e}(t)||d_\eta(t)| \\ &\quad + \frac{\mu\bar{c}^2}{2\rho}|\tilde{\theta}_{n_e}(t)||\check{\zeta}(t)|,\end{aligned}$$

The following result can now be proven.

Theorem 4.1 (ISS of the dynamic estimator): If

Assumption 1 holds, then in an active adaptation interval $t_e(k) \leq t < t_d(k+1)$, given the sinusoidal signal $y(t)$ defined in (2) and the perturbed measurement (1), there exist suitable choices of $\mu \in \mathbb{R}_{>0}$, $\rho \in \mathbb{R}_{>0}$ and L such that $V_{n_e}(t)$ is an ISS Lyapunov function with respect to any bounded disturbance d_η and in turn ISS with respect to bounded measurement disturbance $|d(t)| \leq \bar{d}$. Thus $\tilde{z}(t)$ and $\tilde{\theta}_{n_e}(t)$ are ISS with respect to \bar{d} .

Proof: In view of (26), we immediately have $|\tilde{\theta}(t)| = |\tilde{\theta}_{n_e}(t)|$, which implies $V(t) = V_{n_e}(t)$, and makes it possible to study the time-derivative of $V_{n_e}(t)$ in place of $V(t)$:

$$\begin{aligned}\dot{V}_{n_e}(t) &= \frac{1}{2}(\tilde{z}^\top(t)P\dot{\tilde{z}}(t) + \dot{\tilde{z}}^\top(t)P\tilde{z}(t)) + \tilde{\theta}_{n_e}^\top(t)\dot{\tilde{\theta}}_{n_e}(t) \\ &\quad + \frac{g}{2}(\check{\zeta}^\top(t)P\dot{\check{\zeta}}(t) + \dot{\check{\zeta}}^\top(t)P\check{\zeta}(t)).\end{aligned}\quad (34)$$

By letting $\bar{l} \triangleq \|L\|$, $\underline{q} \triangleq \min \text{eig}(Q)$, $\bar{p} \triangleq \max \text{eig}(P)$, after some algebra, $\dot{V}(t)$ can be bounded as follows:

$$\begin{aligned}\dot{V}_{n_e}(t) &\leq -\underline{q}|\tilde{z}(t)|^2 - g\underline{q}|\check{\zeta}(t)|^2 - \mu\delta|\tilde{\theta}_{n_e}(t)|^2 \\ &\quad + \bar{p}\bar{l}|\tilde{z}(t)||d_\eta(t)| + \bar{p}|\tilde{z}(t)|^2|\tilde{\theta}(t)| + \bar{p}\bar{x}|\tilde{z}(t)||\tilde{\theta}(t)| \\ &\quad + \bar{p}\bar{\theta}^*|\tilde{z}(t)|^2 + \mu\bar{p}\bar{c}^2|\tilde{z}(t)|^2 + \mu\bar{p}\bar{c}|\tilde{z}(t)||d_\eta(t)| \\ &\quad + \mu\frac{\bar{c}}{2\rho}|\tilde{\theta}_{n_e}(t)||d_\eta(t)| + \mu\frac{\bar{c}^2}{2\rho}|\tilde{\theta}_{n_e}(t)||\check{\zeta}(t)| \\ &\quad + g\bar{p}\bar{l}|\check{\zeta}(t)||d_\eta(t)| + g\bar{p}\bar{\theta}^*|\tilde{z}(t)||\check{\zeta}(t)|.\end{aligned}$$

In view of the inequality $|\tilde{\theta}_{n_e}(t)| = |\tilde{\theta}(t)| \leq 2\bar{\theta}^*$ and by rearranging the above inequality to put in evidence the square monomial and the binomial terms, we get:

$$\begin{aligned}\dot{V}_{n_e}(t) &\leq -(q - \mu\bar{p}\bar{c}^2 - 3\bar{p}\bar{\theta}^*)|\tilde{z}(t)|^2 + \bar{p}(\bar{l} + \mu\bar{c})|\tilde{z}(t)||d_\eta(t)| \\ &\quad - \frac{g\underline{q}}{2}|\check{\zeta}(t)|^2 - \frac{g\underline{q}}{4}|\check{\zeta}(t)|^2 + g\bar{p}\bar{\theta}^*|\tilde{z}(t)||\check{\zeta}(t)| \\ &\quad - \frac{g\underline{q}}{4}|\check{\zeta}(t)|^2 + g\bar{p}\bar{l}|\check{\zeta}(t)||d_\eta(t)| - \frac{\mu\delta}{2}|\tilde{\theta}_{n_e}(t)|^2 \\ &\quad - \frac{\mu\delta}{6}|\tilde{\theta}_{n_e}(t)|^2 + \bar{p}\bar{x}|\tilde{z}(t)||\tilde{\theta}_{n_e}(t)| - \frac{\mu\delta}{6}|\tilde{\theta}_{n_e}(t)|^2 \\ &\quad + \mu\frac{\bar{c}}{2\rho}|\tilde{\theta}_{n_e}(t)||d_\eta(t)| - \frac{\mu\delta}{6}|\tilde{\theta}_{n_e}(t)|^2 + \mu\frac{\bar{c}^2}{2\rho}|\tilde{\theta}_{n_e}(t)||\check{\zeta}(t)|.\end{aligned}$$

Now, we complete the squares, thus obtaining

$$\begin{aligned} \dot{V}_{n_e}(t) &\leq -\frac{\mu\delta}{2}|\tilde{\theta}_{n_e}(t)|^2 - \left(\frac{g\underline{q}}{2} - \frac{3\mu\bar{c}^4}{8\rho^2\delta}\right)|\tilde{\zeta}(t)|^2 \\ &\quad - \left[\frac{(q - \mu\bar{p}\bar{c}^2 - 3\bar{p}\bar{\theta}^*)}{2} - \frac{g}{\underline{q}}\bar{p}^2(\bar{\theta}^*)^2 - \frac{3(\bar{p}\bar{x})^2}{2\mu\delta}\right]|\tilde{z}(t)|^2 \\ &\quad + \left[\frac{\bar{p}^2(\bar{l} + \mu\bar{c})^2}{2(q - \mu\bar{p}\bar{c}^2 - 3\bar{p}\bar{\theta}^*)} + \frac{3\mu\bar{c}^2}{8\rho^2\delta} + \frac{g}{\underline{q}}\bar{p}^2\bar{l}^2\right]|d_\eta(t)|^2. \end{aligned}$$

Finally, the following inequality can be established:

$$\dot{V}_{n_e}(t) \leq -\beta_1 [V_{n_e}(t) - \gamma_1(\bar{d}_\eta)], \quad (35)$$

where

$$\beta_1 \triangleq 2 \min \left\{ \frac{(q - \mu\bar{p}\bar{c}^2 - 3\bar{p}\bar{\theta}^*)}{2\bar{p}} - \frac{g}{\underline{q}}\bar{p}^2(\bar{\theta}^*)^2 - \frac{3\bar{x}^2\bar{p}}{2\mu\delta}, \frac{\mu\delta}{2}, \frac{q}{2\bar{p}} - \frac{3\mu\bar{c}^4}{8\rho^2\delta\bar{p}} \right\} \quad (36)$$

and

$$\gamma_1(s) \triangleq \frac{1}{\beta_1} \left[\frac{\bar{p}^2(\bar{l} + \mu\bar{c})^2}{2(q - \mu\bar{p}\bar{c}^2 - 3\bar{p}\bar{\theta}^*)} + \frac{3\mu\bar{c}^2}{8\rho^2\delta} + \frac{g}{\underline{q}}\bar{p}^2\bar{l}^2 \right] s^2, \quad \forall s \in \mathbb{R}_{\geq 0}. \quad (37)$$

Hence, the proof is concluded iff

$$\beta_1 > 0. \quad (38)$$

In view of (38), all the components involved in (36) should be positive, wherein $\mu\delta/2 > 0$ can be immediately verified by choosing a positive μ . Now, we set the excitation threshold δ and the Q matrix arbitrarily, determining q . Then, letting $\bar{p} \leq \mu$, we determine a sufficient condition to ensure the positiveness of the first term in (36):

$$\frac{(q - \mu^2\bar{c}^2 - 3\mu\bar{\theta}^*)}{2} - \mu^2\frac{g}{\underline{q}}(\bar{\theta}^*)^2 - \mu\frac{3\bar{x}^2}{2\delta} > 0. \quad (39)$$

Being the Lyapunov parameter $g > 0$ arbitrary, let us fix $g = 1$ for simplicity. At this point, with any fixed regularization parameter $\rho \in \mathbb{R}_{>0}$ (we do not pose limits on ρ now) we can always determine a sufficiently small value of μ for which the inequality holds true. Next, by suitably allocating the poles, we compute the output-injection gain L that realizes the needed \bar{p} . Finally, to render β_1 strict-positive, we choose a sufficient large ρ such that

$$\frac{q}{2\bar{p}} - \frac{3\mu\bar{c}^4}{8g\bar{p}\rho^2\delta} > 0.$$

B. Total dis-excitation phase

Clearly, it is important to show that the estimation error remains bounded also during the time-intervals in which no excitation is present (e.g., $t_d(k) \leq t < t_e(k)$) as illustrated in Fig. 1). This is carried out in the following result.

Lemma 4.1 (Boundedness in dis-excitation phase):

Consider an arbitrary dis-excitation interval $t_d(k) \leq t < t_e(k)$

in which $E_{n_e}(t) = \emptyset$. Then, under the same choices of $\mu \in \mathbb{R}_{>0}$, $\rho \in \mathbb{R}_{>0}$ and L as in Theorem 4.1, $V(t)$ is an ISS Lyapunov function with respect to $d(t)$ (where $|d(t)| \leq \bar{d}$) and with respect to $V(t_d(k))$.

Proof: In the considered dis-excitation scenario, the estimation is totally unexcited in all directions, i.e. $\sum_{i=1}^n \psi_i(t) = 0$, $\forall t \geq t_d(k) > 0$, thus yielding $\dot{\tilde{\theta}}(t) = 0_{n \times 1}$, and $\tilde{\theta}(t) = \tilde{\theta}(\bar{t}^-)$. In this respect, the time-derivative of the Lyapunov function $V(t)$ satisfies

$$\begin{aligned} \dot{V}(t) &\leq -(q - 3\bar{p}\bar{\theta}^*)|\tilde{z}(t)|^2 + \bar{p}\bar{l}|\tilde{z}(t)||d_\eta(t)| \\ &\quad - \frac{g\underline{q}}{2}|\tilde{\zeta}(t)|^2 - \frac{g\underline{q}}{4}|\tilde{\zeta}(t)|^2 + g\bar{p}\bar{\theta}^*|\tilde{z}(t)||\tilde{\zeta}(t)| \\ &\quad - \frac{g\underline{q}}{4}|\tilde{\zeta}(t)|^2 + g\bar{p}\bar{l}|\tilde{\zeta}(t)||d_\eta(t)| + \bar{p}\bar{x}|\tilde{z}(t)||\tilde{\theta}(t)|. \end{aligned}$$

Applying the inequality $|\tilde{\theta}(t_d(k))|^2 \leq 2V(t_d(k))$, $\forall t \geq t_d(k)$, we have:

$$\begin{aligned} \dot{V}(t) &\leq -(q - 3\bar{p}\bar{\theta}^*)|\tilde{z}(t)|^2 + \bar{p}\bar{l}|\tilde{z}(t)||d_\eta(t)| \\ &\quad - \frac{g\underline{q}}{2}|\tilde{\zeta}(t)|^2 - \frac{g\underline{q}}{4}|\tilde{\zeta}(t)|^2 + g\bar{p}\bar{\theta}^*|\tilde{z}(t)||\tilde{\zeta}(t)| \\ &\quad - \frac{g\underline{q}}{4}|\tilde{\zeta}(t)|^2 + g\bar{p}\bar{l}|\tilde{\zeta}(t)||d_\eta(t)| \\ &\quad - |\tilde{\theta}(t)|^2 + 2V(t_d(k)) + \bar{p}\bar{x}|\tilde{z}(t)||\tilde{\theta}(t)|. \end{aligned}$$

By completing squares, we obtain the following upper bound for $\dot{V}(t)$:

$$\begin{aligned} \dot{V}(t) &\leq -\left[\frac{(q - 3\bar{p}\bar{\theta}^*)}{2} - \frac{g}{\underline{q}}\bar{p}^2(\bar{\theta}^*)^2 - \frac{3(\bar{p}\bar{x})^2}{2}\right]|\tilde{z}(t)|^2 \\ &\quad - \frac{5}{6}|\tilde{\theta}(t)|^2 - \frac{g\underline{q}}{2}|\tilde{\zeta}(t)|^2 + 2V(t_d(k)) \\ &\quad + \left[\frac{\bar{p}^2\bar{l}^2}{2(q - 3\bar{p}\bar{\theta}^*)} + \frac{g}{\underline{q}}\bar{p}^2\bar{l}^2\right]|d_\eta(t)|^2 \end{aligned}$$

and hence, after some algebra, it follows that

$$\dot{V}(t) \leq -\beta_0(V(t) - L_0V(t_d(k)) - \gamma_0(\bar{d}_\eta(t))) \quad (40)$$

where $L_0 \triangleq 2/\beta_0$,

$$\beta_0 \triangleq 2 \min \left\{ \frac{(q - 3\bar{p}\bar{\theta}^*)}{2\bar{p}} - \frac{g}{\underline{q}}\bar{p}^2(\bar{\theta}^*)^2 - \frac{3\bar{p}\bar{x}^2}{2}, \frac{5}{6}, \frac{q}{2\bar{p}} \right\}$$

and

$$\gamma_0(s) \triangleq \frac{1}{\beta_0} \left[\frac{\bar{p}^2\bar{l}^2}{2(q - 3\bar{p}\bar{\theta}^*)} + \frac{g}{\underline{q}}\bar{p}^2\bar{l}^2 \right] s^2, \quad \forall s \in \mathbb{R}_{\geq 0}.$$

It is immediate to show that $\beta_1 > 0$ implies $\beta_0 > 0$ through a suitable design of μ , ρ and the observer gain L (see the proof taken in Section IV-A), thus concluding the proof. ■

Remark 4.1 (Parameter tuning): In view of (35), (36) and (37), some tuning guidelines for the parameters of the proposed estimator can be concluded. To avoid the increase of the worst-case sensitivity to bounded noises, instead of using a low value of \bar{p} that leads high-gain output injection through L , and high values of \bar{l} and γ_1 correspondingly, we can set $\bar{p} = \mu$ and increase the regularization parameter ρ . Moreover, ■

the tuning criterion of ρ and μ is subject to a typical trade-off between accuracy and convergence speed. For example, a larger ρ or a smaller μ can result in more accuracy estimates at the price of slower convergence speed.

C. Robustness Under Alternate Switching

At this stage, the stability of the adaptive observer under alternate switching is characterized by linking the results obtained for the two excitation phases. Thanks to the Gronwall-Bellman lemma, we will be able to prove that the alternate occurrence of active identification phases and poorly excited phases may yield to convergence provided that the active identification phases have a sufficient duration.

Theorem 4.2: Under the same assumptions of Theorem 4.1, consider the adaptive observer (12), (16), (17), (19) equipped with the excitation-based switching strategy defined in (25). Then, the discrete dynamics induced by sampling the adaptive observer in correspondence of the switching transitions is ISS with respect to the disturbance d_η and in turn ISS with respect to bounded measurement disturbance $|d(t)| \leq \bar{d}$ if the excitation phases last longer than $\beta_1^{-1} \ln(L_0)$.

Proof: By the Gronwall-Bellman Lemma, the value of the Lyapunov function (40) within the dis-excitation intervals can be bounded as follows:

$$\begin{aligned} V(t) &\leq V(t_d(k)) + \left(1 - e^{-\beta_0(t-t_d)}\right) \\ &\quad \times \left(L_0 V(t_d(k)) + \gamma_0(\bar{d}_\eta) - V(t_d(k))\right), \\ &\quad \forall t \in [t_d(k), t_e(k)], \forall k \in \mathbb{Z}^+. \end{aligned}$$

Instead, during the excitation phases, the Lyapunov function (35) can be bounded as

$$\begin{aligned} V(t) &\leq V(t_e(k)) + \left(1 - e^{-\beta_1(t-t_e(k))}\right) \\ &\quad \times \left(\gamma_1(\bar{d}_\eta) - V(t_e(k))\right), \\ &\quad \forall t \in [t_e(k), t_d(k+1)], \forall k \in \mathbb{Z}^+. \end{aligned}$$

In order to link the two modes of behaviour, let us denote by $V_k = V(t_d(k))$ the value of the Lyapunov function sampled at the k -th transition to dis-excitement, occurring at time $t_d(k)$ (or equivalently, at the end of the $(k-1)$ -th active identification phase).

Due to the poor excitation during the interval $[t_d(k), t_e(k)]$, at the transition time $t_e(k)$ we can establish the (possibly conservative) bound

$$V(t_e(k)) \leq L_0 V_k + \gamma_0(\bar{d}_\eta).$$

Such a bound holds for any duration the disexcitation phase. For any subsequent active identification time $t = t_e(k) + \Delta t$ with $\Delta t < t_d(k+1) - t_e(k)$, we get the inequality:

$$\begin{aligned} V(t) &\leq V(t_e(k)) + \left(1 - e^{-\beta_1(t-t_e(k))}\right) \left(\gamma_1(\bar{d}_\eta) - V(t_e(k))\right) \\ &= \gamma_1(\bar{d}_\eta) - e^{-\beta_1(t-t_e(k))} \gamma_1(\bar{d}_\eta) + e^{-\beta_1(t-t_e(k))} V(t_e(k)) \\ &\leq \gamma_1(\bar{d}_\eta) - e^{-\beta_1(t-t_e(k))} \gamma_1(\bar{d}_\eta) \\ &\quad + e^{-\beta_1(t-t_e(k))} \left(\gamma_0(\bar{d}_\eta) + L_0 V_k\right) \\ &= \gamma_1(\bar{d}_\eta) + e^{-\beta_1 \Delta t} \left(\gamma_0(\bar{d}_\eta) - \gamma_1(\bar{d}_\eta) + L_0 V_k\right). \end{aligned}$$

Now, let us arbitrarily set $0 < \kappa < 1$ and let $\Delta T_e = -\beta_1^{-1} \ln(L_0^{-1} \kappa)$. If the active identification phase is long

enough to verify the inequality $t_d(k+1) - t_e(k) > \Delta T_e$, then we can guarantee the following difference bound on the discrete (sampled) Lyapunov function sequence:

$$V_{k+1} \leq \gamma_1(\bar{d}_\eta) + \frac{\kappa}{L_0} \left(\gamma_0(\bar{d}_\eta) - \gamma_1(\bar{d}_\eta)\right) + \kappa V_k$$

which can be rewritten in the following compact form:

$$V_{k+1} - V_k \leq -(1 - \kappa)V_k + \gamma(\bar{d}_\eta),$$

where $\gamma(s) = \gamma_1(s) + \kappa L_0^{-1} (\gamma_0(s) - \gamma_1(s))$, $\forall s \geq 0$.

We can conclude that V_k is a discrete ISS Lyapunov function for the sampled sequence, with samples taken at the end of the excitation phases assumed always to last longer than $\beta_1^{-1} \ln(L_0)$.

Now, we recover the ISS properties for the continuous-time system by studying the inter-sampling behaviour of $V(t)$. Let $k(t)$, $\forall t > 0$ denote the index of the current time-window: $k(t) = k : t \in [t_d(k), t_d(k+1))$ and consider two positive constants $\Delta t_1, \Delta t_2$, such that $\Delta t_1 \leq t_e(k) - t_d(k)$, $\Delta t_2 \leq t_d(k+1) - t_e(k)$. Between two samples, the Lyapunov function is bounded by:

$$\begin{aligned} V(t) &\leq \\ &\max_{\Delta t_1 \in \mathbb{R}_{\geq 0}} \left\{ V_{k(t)} + (1 - e^{-\beta_0 \Delta t_1}) (L_0 V_{k(t)} + \gamma_0(\bar{d}_\eta) - V_{k(t)}) \right\} \\ &+ \max_{\Delta t_2 \in \mathbb{R}_{\geq 0}} \left\{ \gamma_1(\bar{d}_\eta) - e^{-\beta_1 \Delta t_2} (\gamma_1(\bar{d}_\eta) - \gamma_0(\bar{d}_\eta) - L_0 V_{k(t)}) \right\} \\ &\leq [(1 + L_0)V_{k(t)} + \gamma_0(\bar{d}_\eta)] + [\gamma_1(\bar{d}_\eta) + \gamma_0(\bar{d}_\eta) + L_0 V_{k(t)}] \\ &= (1 + 2L_0)V_{k(t)} + \gamma_1(\bar{d}_\eta) + 2\gamma_0(\bar{d}_\eta). \quad (41) \end{aligned}$$

If we let $k(t) \xrightarrow[t \rightarrow \infty]{} \infty$ (i.e., an infinite number of active identification phases occurs asymptotically or a single excitation phase lasts indefinitely), then the estimation error in the inter-sampling times converges to a region whose radius depends only on the assumed disturbance bound. ■

V. SIMULATION AND EXPERIMENTAL RESULTS

A. Simulation Results

In this subsection, some numerical examples are given to illustrate the effectiveness of the proposed multi-sinusoidal estimator. The Forward-Euler discretization method with sampling period $T_s = 3 \times 10^{-4}$ s is employed in all simulations.

Example 1: In this example, we compare the proposed method with two techniques available from the literature: the adaptive observer methods [30], [32] and the parallel AFLL method [22], all fed by the following signal composed by two sinusoids:

$$y(t) = \sin(2t) + \sin(5t).$$

All the methods are initialized with the same initial conditions $\hat{\omega}_1(0) = 3$ and $\hat{\omega}_2(0) = 4$. Method [30] is tuned with: $\gamma_1 = \gamma_2 = 8 \times 10^3$, $k = 1$, $d_2 = 9$, $d_3 = 27$, $d_4 = 27$, while the adaptive observer [32] is tuned with $\lambda_0 = \lambda_3 = 4$, $\lambda_1 = \lambda_2 = 6$, $k_1 = k_2 = 20$. The FLL method [22] is set to: $K_{s_1} = K_{s_2} = 1$, $\gamma_{s_1} = 0.3$, $\gamma_{s_2} = 0.5$, $\omega_{s_1} = 3$, $\omega_{s_2} = 4$. The tuning gains of the proposed method are chosen as: $a_1 = 0$, $a_2 = -0.5$, $F_f = -5$, $B_f = 4.5$, $\mu = 6$, $\rho = 0.2$, $\mu_A = 0.15$ with the poles placed at $(-2, -0.7, -0.5, -0.2)$. The simulation results are reported in Fig.3.

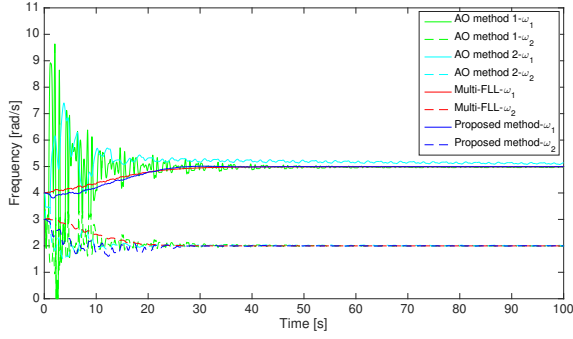


Fig. 3. Time-behavior of the estimated frequencies obtained by using the proposed method (blue) compared with the time behaviors of the estimated frequencies by [30] (green), [22] (red) and [32] (yellow).

It is worth noting from Fig. 3 that all the estimators succeed in detecting the frequencies in a noise-free scenario, after a similar transient behavior (through a suitable choice of the tuning gains), though method [30] is subject to a slightly larger overshoot.

Let us now consider the input signal $y(t)$ corrupted by a bounded noise $d(t)$ uniformly distributed in the interval $[-0.25, 0.25]$. As shown in Fig. 4, the stationary performance of methods [30] and [32] deteriorate due to the injection of the perturbation, while the proposed method and the FLL tool [22] exhibit a relatively better noise immunity.

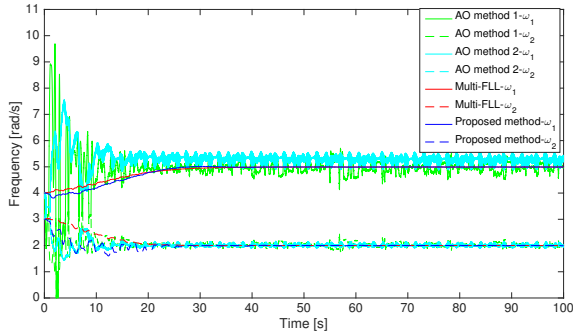


Fig. 4. Time-behavior of the estimated frequencies by using the proposed method (blue) compared with the time behaviors of the estimated frequencies by the method [30] (green), [22] (red) and [32] (yellow).

The estimated amplitudes obtained by [22] are compared with the outcomes of the proposed adaptive observer in Fig. 5 (we only pick two methods that perform better in frequency estimation). Thanks to the adaptive scheme (11), the proposed method offers a smoother transitory and improves the steady state behavior in presence of an external disturbance $d(t)$, at the cost of a slower convergence speed.

Moreover, resorting to the estimated amplitudes and phases, the input is reconstructed by the next equation

$$\hat{y}(t) = \hat{A}_1(t) \sin \hat{\varphi}_1(t) + \hat{A}_2(t) \sin \hat{\varphi}_2(t).$$

Some periods of the estimates are plotted for observation in Figure 6, where the accuracy of the phase estimation is verified.

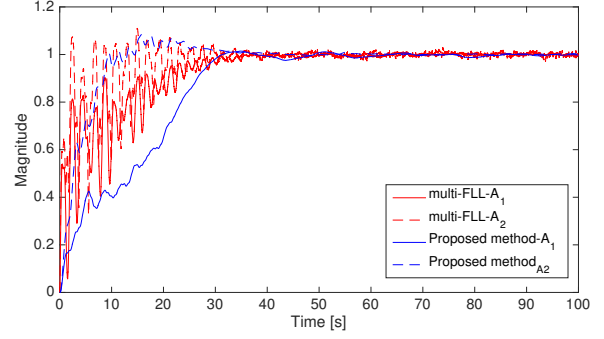


Fig. 5. Time-behavior of the estimated amplitudes by using the proposed method (blue) compared to the estimates by the method [22] (red).

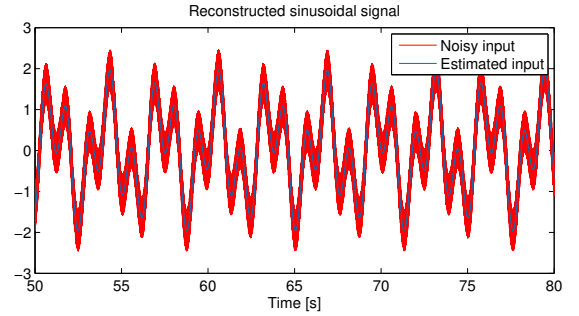


Fig. 6. Estimated sinusoidal signal by the proposed AFP method.

Example 2: In order to evaluate the performance of the method in presence of a dc offset and of a partial dis-excitation, consider a biased signal consisting of two sine waves that turn into a pure single sinusoid after a certain time instant:

$$\hat{y}(t) = 4 \sin(3t) + A_2(t) \sin(2t) + 1 + d(t)$$

where $A_2(t)$ obeys a step-wise change: $A_2(t) = 3, 0 \leq t < 120$, $A_2(t) = 0, t \geq 120$ and $d(t)$ is a random noise with the same characteristics as in the previous example. The behavior of the proposed estimator is recorded in Figs. 7-9 with the tuning gains chosen as follows: $F_f = -6$, $B_f = 6$, $a_1 = -2$, $a_2 = -1$, $\mu = 70$, $\rho = 0.3$, $\mu_A = 0.1$, $\bar{\delta} = 3 \times 10^{-4}$, $\underline{\delta} = 3 \times 10^{-5}$ and the poles' location $[-0.6, -0.5, -0.3, -1, -10]$.

More specifically, in Fig. 7 the excitation signals $\lambda_1(\Phi(\Xi(t)))$, $\lambda_2(\Phi(\Xi(t)))$ are shown together with the correspondent switching signals $\psi_1(t)$, $\psi_2(t)$, to enhance the fact that the proposed methodology allows to check in real-time the excitation level for the single components, thus allowing to possibly stop the parameter adaptation in case of poor excitation.

Moreover, it follows from Fig. 8 and Fig. 9 that all the initialized parameters including the offset are successfully estimated. After time $t = 120s$, the system is characterized by over-parametrization. The vanishing of the second sinusoid is captured by the associated amplitude estimate, that fades to 0 eventually, though the frequency estimate is non-zero. Conversely, the parameters of the excited sinusoidal components remain in a neighborhood of the true ones.

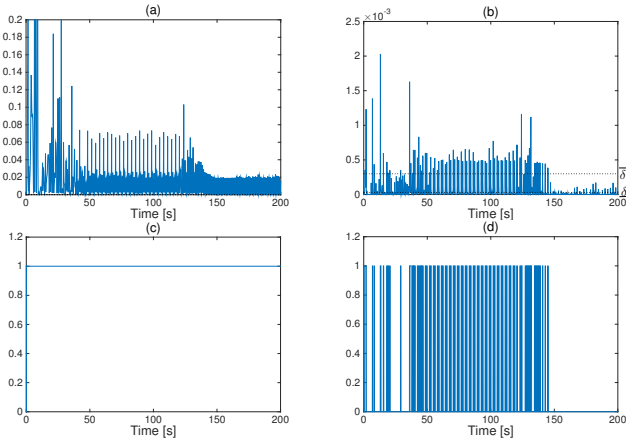


Fig. 7. (a) Excitation level $\lambda_1(\Phi(\Xi(t)))$; (b) Excitation level $\lambda_2(\Phi(\Xi(t)))$; (c) Switching signal $\psi_1(t)$; (d) Switching signal $\psi_2(t)$.

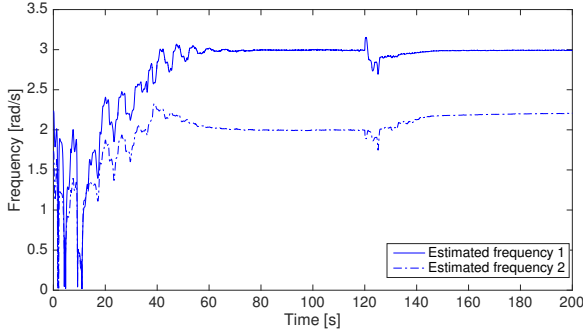


Fig. 8. Time-behavior of the estimated frequencies by using the proposed method.

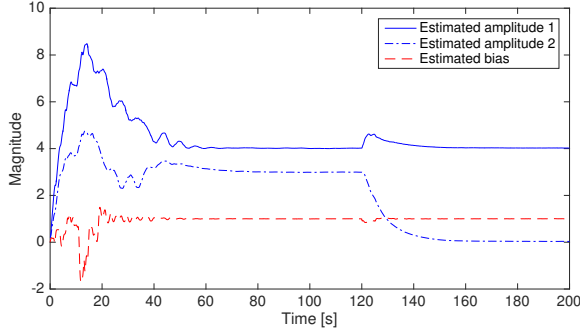


Fig. 9. Time-behavior of the estimated amplitudes (blue) and the estimated bias (red) by using the proposed method.

Example 3: In the example, we consider a different scenario to show the effectiveness of the proposed method in the presence of step-changing frequencies. Let

$$y(t) = \sin \omega_1(t)t + \sin \omega_2(t)t + d(t).$$

where $\omega_1(t)$ and $\omega_2(t)$ are time-varying frequencies, namely: $\omega_1(t) = 2$ rad/s, $0 \leq t < 70$, $\omega_1(t) = 3$ rad/s, $t \geq 70$, $\omega_2(t) = 5$ rad/s, $0 \leq t < 70$, $\omega_2(t) = 4.5$ rad/s, $t \geq 70$. The disturbance $d(t)$ is a bounded signal with the same characteristics as in the previous example. The tunable parameters are given by: $a_1 = 0$, $a_2 = -0.5$, $F_f = -5$, $B_f =$

4.5 , $\mu = 6$, $\rho = 0.2$, $\mu_A = 0.15$ with the poles placed at $(-2, -0.7, -0.5, -0.2)$.

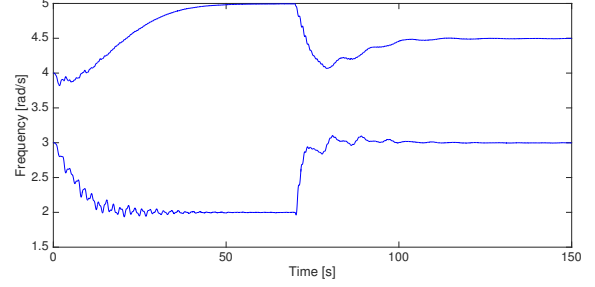


Fig. 10. Time-behavior of the estimated frequencies by using the proposed method.

It is worth noting from Fig. 10 that the proposed adaptive observer succeeded in tracking sudden changes of frequency in a noisy environment.

B. Experimental Results

In order to investigate the behavior of the proposed method in a real-time digital implementation, we have deployed the proposed algorithm on a dSpace board connected to a programmable electrical signal generator (see Fig. 11): *Tektronix AFG3102 dual channel function generator*, which produces the voltage signal

$$y(t) = 4 \sin(7t) + 2 \sin(5t)$$

affected by additive random noise. Fig. 12 shows some periods of the noisy sinusoidal signal generated by the programmable source. Computation burden is one of the most important aspects of implementation in practice. For the sake of simplicity, all the dynamic equations of the estimator are discretized by the forward Euler method, avoiding an excessive load for the dSpace system. The parameters of the estimator (4th order for two frequencies) is set to $a_1 = 0$, $a_2 = -1$, $F_f = -2$, $B_f = 1$, $\mu = 20$, $\rho = 1$, $\mu_A = 0.2$ with the poles placed at $(-0.7, -0.4, -0.5, -1)$.

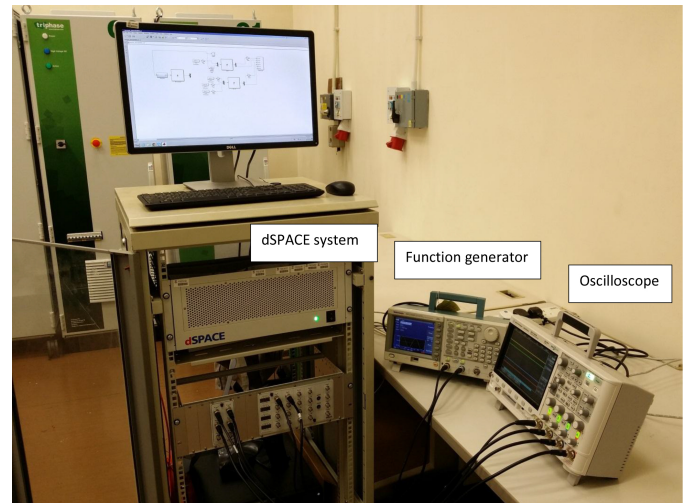


Fig. 11. The experimental setup.

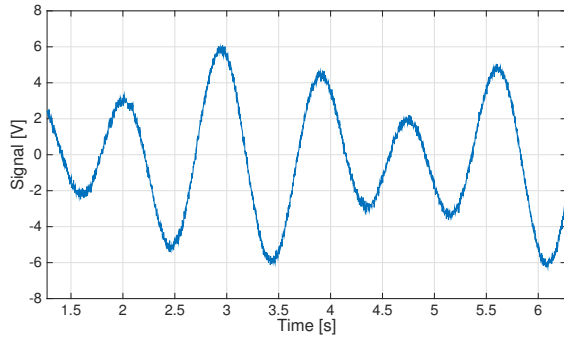


Fig. 12. A real-time noisy signal generated by the electrical signal generator.

The dSpace board computes the estimates in real-time with a fixed sampling rate of 10KHz based on the Matlab/Simulink platform. The results are captured by an oscilloscope with 4 channels respectively allocated to dual frequencies and amplitudes. The measured signals are then imported in Matlab for carrying out the post-analysis. As shown in Fig. 13 and 14, the estimator is capable to gather the frequency and amplitude contents with great accuracy, despite the unavoidable measurement noise due the limitation of the measurement devices.

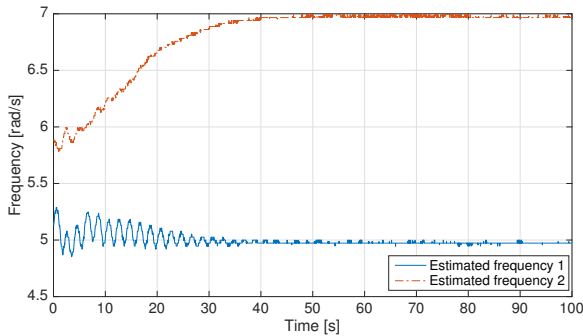


Fig. 13. Real-time frequency detection of a signal made up of two sinusoids by the proposed method

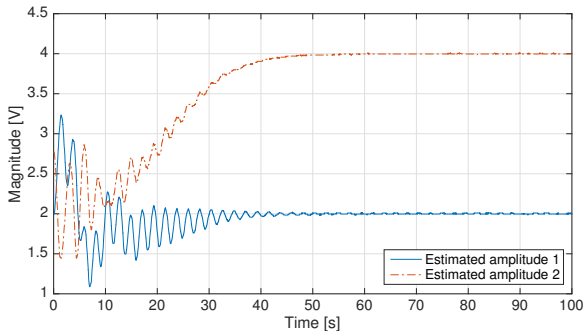


Fig. 14. Real-time amplitude detection of a single with two frequency contents by using the proposed method.

VI. CONCLUDING REMARKS

In this paper, a new adaptive-observer based technique [35] is proposed for estimating the amplitudes, frequencies

and phases of the sinusoids composing a multi-sinusoidal signal, in presence of bias and bounded additive disturbances. Compared to other adaptive observer methods that estimate the characteristic polynomial's coefficients of the signal-generator system, the proposed algorithm allows for the direct adaptation of the squared-frequencies of the components. Thanks to the excitation-based switching dynamics that disables the adaptation under poor excitation conditions in real-time, the proposed estimator is proven to be ISS with respect to bounded disturbances and overparametrization. The tuning criteria of the adaptation parameters of the estimator are obtained analytically as a result of the ISS based analysis. The effectiveness of the proposed algorithm has been shown by extensive simulations and real-time experiments.

Future research efforts will be devoted to extend the analysis and the algorithm to the important case of tracking time-varying changes of the frequencies of the multi-sinusoidal signals. Moreover, challenging practical use-cases will be dealt with such as, for example, estimation of vibrations in power generators and estimation in sea-wave analysis contexts.

REFERENCES

- [1] A. A. P. Stanislav V. Aranovskiy, Alexey A. Bobtsov and P. A. Gritcenko, "Adaptive filters cascade applied to a frequency identification improvement problem," *International Journal of Adaptive Control and Signal Processing*, pp. 677–689, 2015.
- [2] N. A. Khan and B. Boashash, "Multi-component instantaneous frequency estimation using locally adaptive directional time frequency distributions," *International Journal of Adaptive Control and Signal Processing*, pp. 429–442, 2015.
- [3] G. Pin, "A direct approach for the frequency-adaptive feedforward cancellation of harmonic disturbances," *IEEE Trans. on Signal Processing*, vol. 58, no. 7, pp. 3513–3530, 2010.
- [4] H. Hajimolahoseini, M. R. Taban, and H. Soltanian-Zadeh, "Extended kalman filter frequency tracker for nonstationary harmonic signals," *Measurement*, vol. 45, no. 1, pp. 126–132, 2012.
- [5] L. Hsu, R. Ortega, and G. Damm, "A globally convergent frequency estimator," *IEEE Trans. on Automatic Control*, vol. 44, no. 4, pp. 698–713, 1999.
- [6] M. Mojiri and A. R. Bakhshai, "An adaptive notch filter for frequency estimation of a periodic signal," *IEEE Trans. on Automatic Control*, vol. 49, no. 2, pp. 314–318, 2004.
- [7] M. Karimi-Ghartemani and A. K. Ziarani, "A nonlinear time-frequency analysis method," *IEEE Trans. on Signal Processing*, vol. 52, no. 6, pp. 1585–1595, 2004.
- [8] B. Wu and M. Bodson, "A magnitude/phase-locked loop approach to parameter estimation of periodic signals," *IEEE Trans. on Automatic Control*, vol. 48, no. 4, pp. 612–618, 2003.
- [9] M. Karimi-Ghartemani, S. A. Khajehoddin, P. K. Jain, A. Bakhshai, and M. Mojiri, "Addressing dc component in pll and notch filter algorithms," *IEEE Trans. on Power Electronics*, vol. 27, no. 1, pp. 78–86, 2012.
- [10] G. Fedele and A. Ferrise, "Non adaptive second order generalized integrator for identification of a biased sinusoidal signal," *IEEE Trans. on Automatic Control*, vol. 57, no. 7, pp. 1838–1842, 2012.
- [11] G. Fedele, A. Ferrise, and P. Muraca, "An adaptive quasi-notch filter for a biased sinusoidal signal estimation," in *IEEE International Conference on Control and Automation (ICCA)*, Santiago, 2011, pp. 1060–1065.
- [12] A. A. Pyrkin, A. A. Bobtsov, D. Efimov, and A. Zolghadri, "Frequency estimation for periodical signal with noise in finite time," in *Proc. of the IEEE Conf. on Decision and Control*, Orlando, FL, 2011, pp. 3646–3651.
- [13] A. A. Bobtsov, D. Efimov, A. A. Pyrkin, and A. Zolghadri, "Switched algorithm for frequency estimation with noise rejection," *IEEE Trans. on Automatic Control*, vol. 57, no. 9, pp. 2400–2404, 2012.
- [14] G. Pin, T. Parisini, and M. Bodson, "Robust parametric identification of sinusoidal signals: an input-to-state stability approach," in *Proc. of the IEEE Conf. on Decision and Control*, Orlando, FL, 2011, pp. 6104–6109.

- [15] G. Pin, B. Chen, T. Parisini, and M. Bodson, "Robust sinusoid identification with structured and unstructured measurement uncertainties," *IEEE Trans. on Automatic Control*, vol. 59, no. 6, pp. 1588–1593, 2014.
- [16] B. Chen, G. Pin, and T. Parisini, "Robust parametric estimation of biased sinusoidal signals: a parallel pre-filtering approach," in *Proc. of the IEEE Conf. on Decision and Control*, Los Angeles, 2014.
- [17] X. Guo and M. Bodson, "Frequency estimation and tracking of multiple sinusoidal components," in *Proc. of the IEEE Conf. on Decision and Control*, Maui, Hawaii, USA, 2003.
- [18] G. Pin and T. Parisini, "A direct adaptive method for discriminating sinusoidal components with nearby frequencies," in *Proc. of the IEEE American Control Conference*, O'Farrell Street, San Francisco, CA, USA, 2011, pp. 2994–2999.
- [19] M. Mojiri, M. Karimi-Ghartemani, and A. Bakhshai, "Time-domain signal analysis using adaptive notch filter," *IEEE Trans. on Signal Processing*, vol. 55, no. 1, pp. 85–93, 2007.
- [20] —, "Processing of harmonics and interharmonics using an adaptive notch filter," *IEEE Trans. on Power Delivery*, vol. 25, no. 2, pp. 534–542, 2010.
- [21] M. Karimi-Ghartemani and M. R. Iravani, "Measurement of harmonics/inter-harmonics of time-varying frequencies," *IEEE Trans. on Power Delivery*, vol. 20, no. 1, pp. 23–31, 2005.
- [22] G. Fedele and A. Ferrise, "A frequency-locked-loop filter for biased multi-sinusoidal estimation," *IEEE Trans. on Signal Processing*, vol. 62, no. 5, pp. 1125–1134, 2014.
- [23] G. Obregon-Pulido, B. Castillo-Toledo, and A. Loukianov, "A globally convergent estimator for n frequencies," *IEEE Trans. on Automatic Control*, vol. 47, no. 5, pp. 857–863, 2002.
- [24] X. Xia, "Global frequency estimation using adaptive identifiers," *IEEE Trans. on Automatic Control*, vol. 47, no. 7, pp. 1188–1193, 2002.
- [25] M. Hou, "Estimation of sinusoidal frequencies and amplitudes using adaptive identifier and observer," *IEEE Trans. on Automatic Control*, vol. 52, no. 3, pp. 493–499, 2007.
- [26] B. B. Sharma and I. N. Kar, "Design of asymptotically convergent frequency estimator using contraction theory," *IEEE Trans. on Automatic Control*, vol. 53, no. 8, pp. 1932–1937, 2008.
- [27] A. A. Bobtsov and A. A. Pyrkin, "Cancellation of unknown multiharmonic disturbance for nonlinear plant with input delay," *Int. J. Adapt. Control Signal Process*, vol. 26, no. 4, pp. 302–315, 2012.
- [28] D. Carnevale and A. Astolfi, "A hybrid observer for frequency estimation of saturated multi-frequency signals," in *Proc. of the IEEE Conf. on Decision and Control and European Control Conference*, Orlando, FL, USA, 2011, pp. 2577–2582.
- [29] D. Carnevale, S. Galeani, M. Sassano, and A. Astolfi, "Robust hybrid estimation and rejection of multi-frequency signals," *International Journal of Adaptive Control and Signal Processing*, 2016.
- [30] R. Marino and P. Tomei, "Global estimation of n unknown frequencies," *IEEE Trans. on Automatic Control*, vol. 47, no. 8, pp. 1324–1328, 2002.
- [31] D. Carnevale and A. Astolfi, "A minimal dimension observer for global frequency estimation," in *Proc. IEEE American Control Conference*, Seattle, WA, 2008, pp. 5269–5274.
- [32] M. Hou, "Parameter identification of sinusoids," *IEEE Trans. on Automatic Control*, vol. 57, no. 2, pp. 467–472, 2012.
- [33] B. Chen, G. Pin, W. M. Ng, C. K. Lee, S. Y. R. Hui, and T. Parisini, "An adaptive observer-based switched methodology for the identification of a perturbed sinusoidal signal: Theory and experiments," *IEEE Trans. on Signal Processing*, vol. 62, no. 24, pp. 6355–6365, 2014.
- [34] B. Chen, G. Pin, and T. Parisini, "An adaptive observer-based estimator for multi-sinusoidal signals," in *Proc. IEEE American Control Conference*, Portland, OR, USA, 2014.
- [35] G. Pin, B. Chen, and T. Parisini, "A nonlinear adaptive observer with excitation-based switching," in *Proc. of the 2013 Conference on Decision and Control*, Florence, 2013, pp. 4391–4398.
- [36] G. Tao and P. A. Ioannou, "Persistence of excitation and over-parametrization in model reference adaptive control," *IEEE Trans. on Automatic Control*, vol. 35, no. 2, pp. 254–256, 1990.
- [37] B. Francis and B. Wonham, "The internal model principle of control theory," *Automatica*, vol. 12, no. 5, pp. 457–465, 1976.

PLACE
PHOTO
HERE

Boli Chen received the B. Eng. in electrical and electronic engineering in 2010 from Northumbria University, UK and Nanjing Normal University, China. In 2011, he received his MSc and Ph.D. in control systems from Imperial College London, UK. He is currently working towards his PhD degree at Imperial College London, UK. His research interests include nonlinear estimation, and its application to sinusoidal identification, design of deadbeat identification algorithm and observers.

PLACE
PHOTO
HERE

Gilberto Pin received the Laurea (M.Sc.) degree in Electrical Engineering (with honors) and the Ph.D. in Information Engineering from the University of Trieste, Italy, in 2005 and 2009, respectively. From 2009 to 2012 he was an Automation Engineer at Danieli Automation S.p.A., Italy. Since 2013, he has been a Control Systems Engineer at the R&D Dept. of Electrolux Professional S.p.A., Italy. He is author of several papers published in international conferences and scientific journals concerning systems theory, signal processing methods and control applications. He is a co-recipient of the IFAC Best Application Paper Prize of the Journal of Process Control, Elsevier, for the three-year period 2011–2013. His current research interests include networked control, model predictive control, advanced system identification methods and deadbeat observers design. His activity is also devoted to the industrial application of advanced control techniques

PLACE
PHOTO
HERE

W. M. Ng (MPhil, CEng, MIEE) received the B.Eng. in electronic engineering in 1998, and M.Phil. in 2004, from the City University of Hong Kong, where he is now working toward the Ph.D. at the University of Hong Kong. From 1998 to 2000, he was an Electronic Engineer in the Astec Custom Limited. He worked as an Application Engineer in Ericsson Limited from 2000 to 2003. In 2009, he joined the City University of Hong Kong as a Research Fellow. Since 2011, he has been with Department of Electrical and Electronic Engineering, University of Hong Kong, as a Research Officer. He is author or coauthor of over 10 journal and conference papers. He is the co-inventor of 2 U.S. patents. His current research interests include electromagnetic interference, LED control, gas-discharge lamp, smart grid and wireless power transfer.

PLACE
PHOTO
HERE

S. Y. R. (Ron) Hui (M87-SM94-F03) received his BSc (Eng) Hons at the University of Birmingham in 1984 and a D.I.C. and PhD at Imperial College London in 1987. Presently, he holds the Philip Wong Wilson Wong Chair Professorship at the University of Hong Kong and a Chair Professorship at Imperial College London. He has published over 300 technical papers, including more than 180 refereed journal publications. Over 55 of his patents have been adopted by industry. He is an Associate Editor of the IEEE Transactions on Power Electronics and

IEEE Transactions on Industrial Electronics, and an Editor of the IEEE Journal of Emerging and Selected Topics in Power Electronics. Appointed twice as an IEEE Distinguished Lecturer by the IEEE Power Electronics Society in 2004 and 2006, he won an IEEE Best Paper Award from the IEEE IAS in 2002, and two IEEE Power Electronics Transactions Prize Paper Awards in 2009 and 2010. His inventions on wireless charging platform technology underpin key dimensions of Qi, the world's first wireless power standard, with freedom of positioning and localized charging features for wireless charging of consumer electronics. In Nov. 2010, he received the IEEE Rudolf Chope R&D Award from the IEEE Industrial Electronics Society and the IET Achievement Medal (The Crompton Medal). He is a Fellow of the Australian Academy of Technological Sciences & Engineering and is the recipient of the 2015 IEEE William E. Newell Power Electronics Award.

PLACE
PHOTO
HERE

Thomas Parisini received the Ph.D. degree in Electronic Engineering and Computer Science in 1993 from the University of Genoa. He was with Politecnico di Milano and since 2010 he holds the Chair of Industrial Control and is Director of Research at Imperial College London. He is a Deputy Director of the KIOS Research and Innovation Centre of Excellence, University of Cyprus. Since 2001 he is also Danieli Endowed Chair of Automation Engineering with University of Trieste. In 2009-2012 he was Deputy Rector of University of Trieste. He

authored or co-authored more than 270 research papers in archival journals, book chapters, and international conference proceedings. His research interests include neural-network approximations for optimal control problems, fault diagnosis for nonlinear and distributed systems, nonlinear model predictive control systems and nonlinear estimation. He is a co-recipient of the IFAC Best Application Paper Prize of the Journal of Process Control, Elsevier, for the three-year period 2011-2013 and of the 2004 Outstanding Paper Award of the IEEE Trans. on Neural Networks. He is also a recipient of the 2007 IEEE Distinguished Member Award. In 2016 he was awarded as Principal Investigator at Imperial of the H2020 European Union flagship Teaming Project *KIOS Research and Innovation Centre of Excellence* led by University of Cyprus. In 2012 he was awarded an ABB Research Grant dealing with energy-autonomous sensor networks for self-monitoring industrial environments. Thomas Parisini currently serves as Vice-President for Publications Activities of the IEEE Control Systems Society and during 2009-2016 he was the Editor-in-Chief of the IEEE Trans. on Control Systems Technology. Since 2017, he is Editor for Control Applications of Automatica. He is also the Chair of the IFAC Technical Committee on Fault Detection, Supervision & Safety of Technical Processes - SAFEPROCESS. He was the Chair of the IEEE Control Systems Society Conference Editorial Board and a Distinguished Lecturer of the IEEE Control Systems Society. He was an elected member of the Board of Governors of the IEEE Control Systems Society and of the European Control Association (EUCA) and a member of the board of evaluators of the 7th Framework ICT Research Program of the European Union. Thomas Parisini is currently serving as an Associate Editor of the Int. J. of Control and served as Associate Editor of the IEEE Trans. on Automatic Control, of the IEEE Trans. on Neural Networks, of Automatica, and of the Int. J. of Robust and Nonlinear Control. Among other activities, he was the Program Chair of the 2008 IEEE Conference on Decision and Control and General Co-Chair of the 2013 IEEE Conference on Decision and Control. Prof. Parisini is a Fellow of the IEEE and of the IFAC.